

High Gain Switched Lc Converter with Lower Output Voltage Ripple for Photovoltaic Applications

Mr. Nandu Dileep¹, Prof. Hemambika V², Prof. Anu George³, Prof Kavitha Issac⁴,
Prof. Eldhose K A⁵, Prof. Binoj Thomas⁶, Prof. Hemambika V⁷

¹PG Scholar Dept of Electrical & Electronics Engg, Mar Athanasius College of Engineering,
Kothamangalam, Kerala, India

^{2,3,4,5,6,7}Dept of Electrical & Electronics Engg, Mar Athanasius College of Engineering
Kothamangalam, Kerala, India

Abstract—High step-up voltage conversion is essential in renewable energy systems to efficiently interface low-voltage sources with high-voltage loads. This project introduces a non-isolated high step-up DC-DC converter that integrates active switched-inductor (ASL) and switched capacitor cell (SCC) techniques. The proposed converter achieves a high voltage gain by strategically configuring capacitors and diodes to interconnect the input and load sides. A key advantage of this design is the division of input current, which reduces inductor size and enhances overall efficiency. Additional benefits include a high step-up ratio at a low duty cycle, reduced voltage ripple and reduced voltage transients across switches. A comprehensive analysis of the converter's operating principles, design equations, and device stress is done. Finally, a laboratory prototype is developed and tested under various operating conditions in continuous conduction mode to validate the theoretical findings. The simulation validates the theoretically claimed analysis. The efficacy of the suggested topology is confirmed by the simulation results. MATLAB/SIMULINK is used to perform the simulation. In the rated state, the maximum efficiency is 93%

Index Terms—Boost Converter, Gain, Efficiency.

I. INTRODUCTION

The primary objective of this project is to design and analyze a Switched LC Converter that effectively reduces voltage stress across semiconductor devices while maintaining high efficiency. This converter aims to enhance power density, decrease component stress, and improve overall system performance, making it a suitable candidate for photovoltaic energy conversion. Through theoretical analysis and simu-

lation studies, the performance of the proposed converter is evaluated and compared with conventional topologies. Additionally, hardware implementation is undertaken to validate the feasibility of the design in real-world conditions. The major strategies for increasing voltage gain include the use of a switched inductor or capacitor cell. Many switched inductors and switched capacitor topologies have been discussed. These are obtained by changing the series and parallel connections of the inductor and capacitor. However, the voltage gain is restricted, and the switch endures high voltage stress equal to the output voltage.

A transformer-less boost converter with less voltage stress is introduced by altering the traditional switching inductor converter. This converter reduces the voltage stress on the switches in comparison to the earlier designs. The main drawback of this converter is the presence of high output voltage ripples at the input side. A detailed analysis of the boost converter in steady-state conditions is carried out.

To overcome the above limitations, a high Gain Switched LC Converter with lower output ripple is introduced. In this paper, a DC-DC converter based switched capacitor and switched-inductor is proposed. The converter can obtain high-gain, wide input voltage range, low voltage stress in addition, there is no extreme duty cycle and the power switches need only one PWM drive signal in circuit topology.

A key advantage of the proposed converter is its high voltage gain, which can be achieved at the same duty cycle as that of the conventional Boost converters. Moreover, the converter design achieves low input voltage ripple due to the dual-switch

architecture combined with input-side inductance. This ripple minimization is especially beneficial for fuel cells, which are sensitive to high-frequency current disturbances.

Additionally, the incorporation of a switched inductor allows for gain expansion without significantly increasing the duty cycle, overcoming the limitations of converters operating in the extreme duty range (close to $D \rightarrow 1$). This ensures stable operation, reduced diode reverse recovery issues, and lower switching losses.

The performance of the modified converter is analyzed in both steady-state and small signal conditions, demonstrating its robustness across wide input voltage variations. Experimental validation using a laboratory prototype confirms the analytical findings. In summary, the proposed converter architecture presents a cost-effective, efficient, and scalable solution for high-gain DC-DC conversion in photovoltaic applications. Its design also holds promise for broader applications including portable energy systems, renewable energy harvesting, and grid-connected distributed energy resources.

II. METHODOLOGY

The High gain switched LC Converter consists of two active switches S_1 & S_2 , four diodes D_0, D_1, D_2 & D_3

, four capacitors C_0, C_1 & C_2 & C_3 , two inductors L_1 & L_2 and a load R . The two power switches S_1 & S_2 operates with same duty ratio. The control signal of the switch S_2 is the same as that of the S_1 .

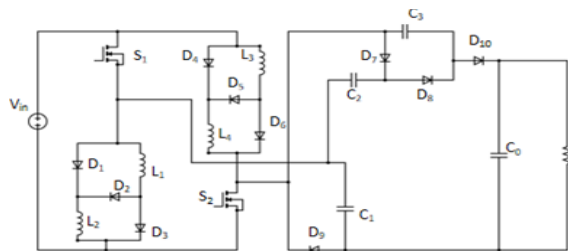


Fig. 1. High Gain switched LC Converter

A. Modes of Operation

The High Gain LC converter operates primarily in two modes.

1. Mode 1: At mode 1, the switches S_1 and S_2 are turned on along with diodes $D_1, D_2, D_3, D_4, D_5, D_6, D_8$ and D_9 and diodes D_7, D_{10} are turned

off. At this moment, the inductor L_1, L_2, L_3 and L_4 are charged through the source. Capacitor C_3 charges capacitor C_2 and V_{in} . Current in both inductors increases linearly. The output capacitor C_0 charges the load. Figure 3.6 shows the operating circuit of mode 1.

2. Mode 2: At mode 2 the switches S_1 and S_2 are turned off along with diodes D_1 and D_4 and, diodes D_0, D_3 and D_5 are turned on. Inductors L_1 - L_4 gets charged by source voltage V_{in} . Capacitors C_1 and C_2 are charged while capacitors C_3 and C_0 are discharged. Figure 3.7 shows the operating circuit of mode 2.

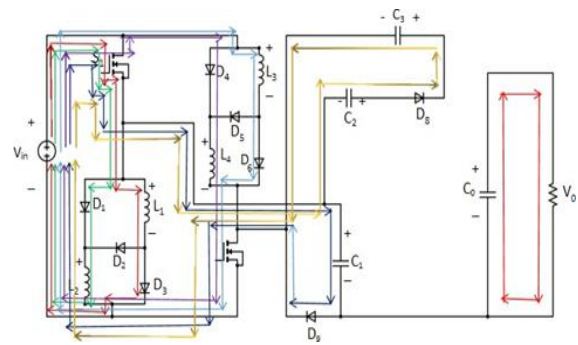


Fig. 2. Operating circuit of of Mode 1

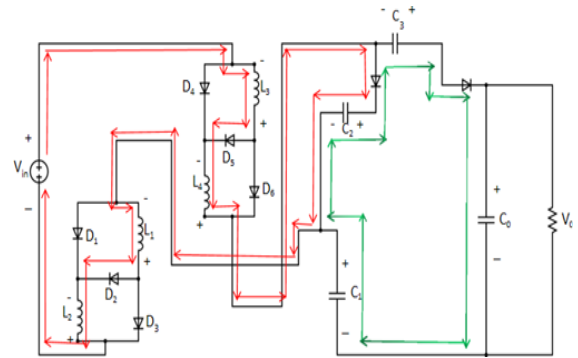


Fig. 3. Operating circuit of of Mode 2

Figure 4 illustrates the theoretical waveforms corresponding to Mode 1 and Mode 2.

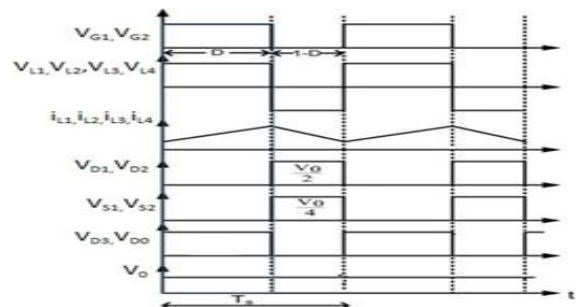


Fig. 4. Theoretical waveform

B. Design of Components

The input voltage is set to $V_{in} = 24\text{ V}$. The output power and output voltage are specified as $P_o = 200\text{ W}$ and $V_o = 200\text{ V}$, respectively. The switching frequency is $f_s = 40\text{ kHz}$, which corresponds to a time period of $T_s = 1/f_s = 25\text{ }\mu\text{s}$. Load resistance can be found by the equation,

$$R_o = \frac{V_o^2}{P_o} = \frac{200^2}{200} = 200\Omega \quad (1)$$

Voltage Gain,

$$M = \frac{V_o}{V_{in}} = \frac{4(1+D)}{1-D}, D = 0.35 \quad (2)$$

The inductors L_1, L_2, L_3 and L_4 are obtained from the following equations.

$$I_{L1} = I_{L2} = I_{L3} = I_{L4} = \frac{I_{IN}}{4} = \frac{V_{in}^2}{2RV_{in}} = \frac{200^2}{2 * 200 * 24} = 5.5/A \quad (3)$$

$$L_1, L_2, L_3, L_4 \geq \frac{V_{IN} * D}{\Delta I_L * f_s} \geq \frac{24 * 0.35}{0.832 * 40 * 10^3} = 250\mu H \quad (4)$$

It is approximated to $250\text{ }\mu\text{H}$

The values of the capacitors are determined using the following equations.

$$C_o \geq \frac{I_o * D}{\Delta V_{C0} * V_{C0} * f_s} \quad (5)$$

C_o is taken as $33\text{ }\mu\text{F}, 250\text{V}$

$$C_1 \geq \frac{I_o}{\Delta V_{C1} * V_{C1} * f_s}$$

C_1 is taken as $63\text{ }\mu\text{F}, 250\text{V}$ (6)

$$C_2 \geq \frac{I_o}{\Delta V_{C2} * V_{C2} * f_s} \quad (7)$$

$$C_3 \geq \frac{I_o}{V_{C3} * \Delta V_{C3} * f_s} \quad (8)$$

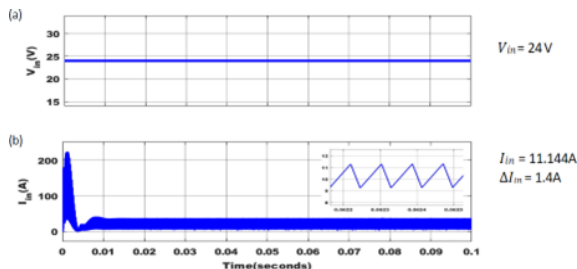


Fig. 5. (a) Input Voltage (V_{in}) and (b) Input Current (I_{in})

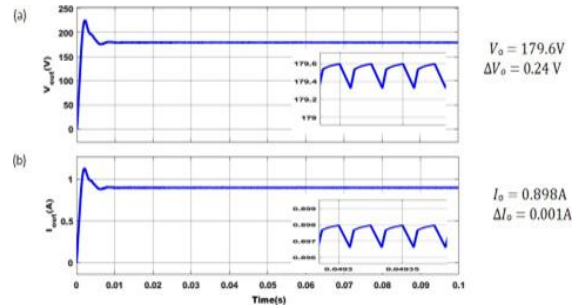


Fig. 6. (a) Output Voltage (V_o) and (b) Output Current (I_o)

III. SIMULATIONS AND RESULTS

Table I Simulation Parameters of Modified Dual-Switch Boost Dc-Dc Converter

Parameters	Value
Input voltage, V_{in}	24 V
Output voltage, V_o	200 V
Output load, R	200 Ω
Switching frequency, f_s	40 kHz
Inductances L_1, L_2, L_3, L_4	$\mu\text{H}, 10\text{A}$
Capacitances C_o, C_2, C_3	33 $\mu\text{F}, 250\text{V}$
Capacitance C_1	63 $\mu\text{F}, 250\text{V}$

In the simulation, a DC input voltage of 24 V was applied to the converter, and it successfully produced an output voltage of 200 V while supplying an output power of 200 W . The waveforms for the input voltage and current are shown in Figure 5, and the output voltage and current waveforms are presented in Figure 6. Based on the input and output voltages, the voltage gain of the converter is calculated as:

$$\text{Voltage Gain} = \frac{V_{out}}{V_{in24}} = \frac{200}{\approx 8.33} \quad (9)$$

Figures 7 and 8 illustrate the gate drive signals and the voltage stresses experienced by the switches in the converter circuit. The measured voltage stress across switch S_1 and S_2 are 50V respectively.

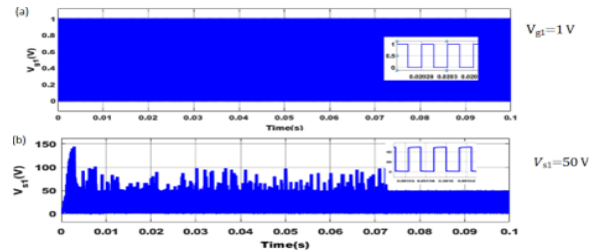


Fig. 7. Gate Pulse (V_{gs1}) and Voltage Stress (V_{s1}) of switch S_1

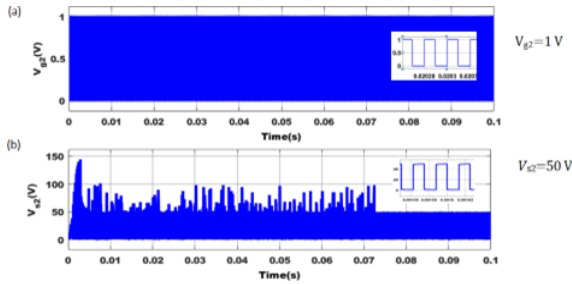


Fig. 8. Gate Pulse (V_{gs2}) and Voltage Stress (V_{s2}) of switch S2

The voltages across the capacitors are measured as $V_{C0} = 179.6$ V, $V_{C1} = 19.48$ V, $V_{C2} = 115$ V and $V_{C3} = 133$ V, as

illustrated in Fig. 8. Fig. 9 presents the current through the inductors L1, L2, L3 and L4, showing that the filter inductance currents i_{L1} , i_{L2} , i_{L3} and i_{L4} are approximately 4.046 A each respectively.

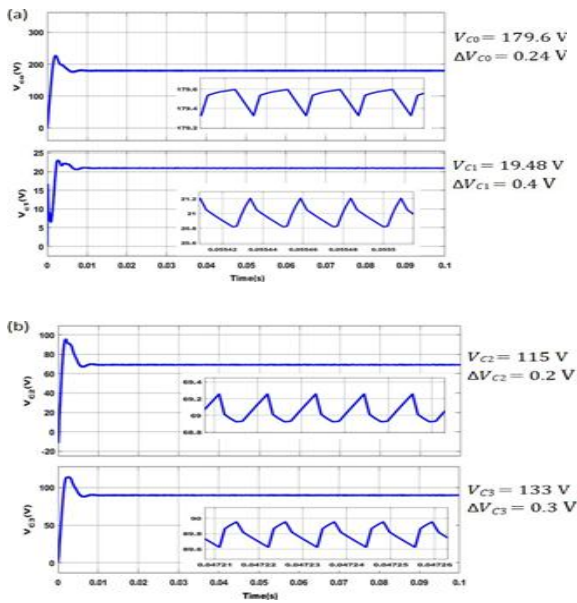


Fig. 9. Voltage across Capacitor (a) V_{C0} and V_{C1} , (b) V_{C2} and V_{C3} ,

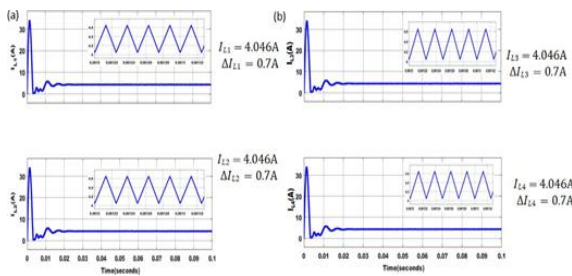


Fig. 10. Current across Inductance (a) i_{L1} and i_{L2} , (b) i_{L3} and i_{L4}

IV. PERFORMANCE ANALYSIS

Efficiency of a power equipment is defined at any load as the ratio of the power output to the power input. The efficiency tells us the fraction of the input power delivered to the load. Here the efficiency vs output power with R load and RL load done for both high gain boost converter (for $R = 200\Omega$) and modified high gain boost converter (for $R = 200\Omega$) and graphs are shown in Figure 5.13. The maximum efficiency of high gain boost converter is around 90% for an output power of 200W for R load and 93% for RL load for an output power of 200W.

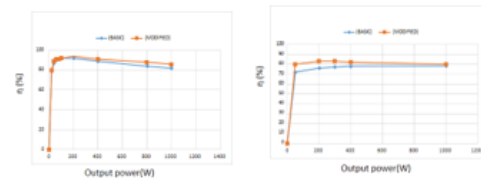


Fig. 11. Efficiency Vs Output Power for (a) R load (b) RL load

The plot of gain of the converter as a function of duty ratio shown in Figure 12. By analyzing the graph, it is clear that the voltage gain increases with duty ratio. It is observed that the voltage gain of high gain switched LC converter increments at a higher rate than the ASL based high step-up boost converter for the same duty ratio.

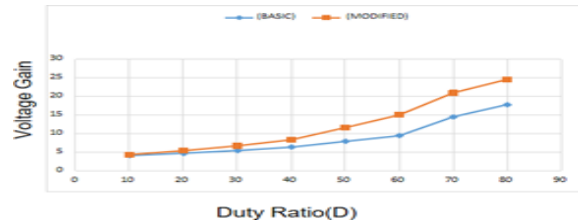


Fig. 12. Voltage gain VS Duty ratio

The plot of output voltage ripple as a function of duty Ratio for High gain LC Converter is shown in figure 13.

Converter	DC-DC Converter [3]	Buck Boost converter [4]	Boost converter [4]	High gain switched LC Converter
No. of Switches	2	1	2	2
No. of Diodes	2	3	9	10
No. of Inductors	2	2	3	4
No. of Capacitors	2	2	4	4

Fig. 13. Output Voltage Ripple VS Duty Ratio

Figure 14 depicts the redesigned LC converter’s output voltage ripple behavior in response to varied switching frequency. The output voltage ripple decreases as the switching frequency increases.

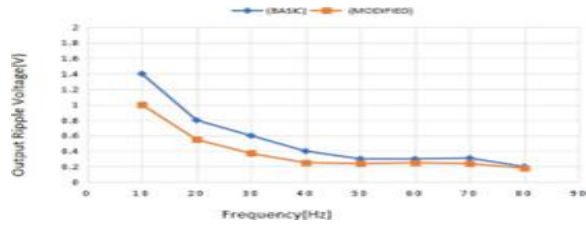


Fig. 14. Output voltage ripple VS frequency

V. COMPARITIVE STUDY

Table 2 compares the ASL Based Boost converter and the proposed version, which operate under identical conditions with an input voltage of 24V and a switching frequency of 40kHz. The results show that, with the duty ratio fixed, the voltage gain in the suggested topology increases dramatically from 8.11 to 11.33. However, this gain comes at the expense of higher output voltage and current ripple, which is a trade-off to consider in actual applications. Table 3 provides a detailed comparison of the components used in the proposed High

Table II Comparison Between Asl Based Boost Dc-Dc Converter& Proposed High Gain Switched Lc Converter

Parameters	ASL Boost Converter	High Gain LC Boost Converter
Voltage Gain	8.33	12.66
Duty Ratio	52%	35%
Maximum Efficiency at R Load	90%	93%
Output Voltage Ripple	0.4V	0.24V
Voltage transient across switches	140V	60V

gain switched LC Converter against those in other converter designs.

Table III Comparison Between High Gain Switched LC Converter & Other Converters

Converter	DC-DC Converter [3]	Buck Boost converter [4]	Boost converter [4]	High gain switched LC Converter
No. of Switches	2	1	2	2
No. of Diodes	2	3	9	10
No. of Inductors	2	2	3	4
No. of Capacitors	2	2	4	4

VI. EXPERIMENTAL SETUP WITH RESULT

The input voltage is lowered to 2V for hardware implementation, and the TMS320F28335 processor is used to generate the switching pulses. The MOSFET IRF3105 switch is utilized. TLP250H, an optocoupler utilized to isolate and shield the microcontroller from harm and to provide the necessary gating to turn on the switches, is used in the implementation of the driver circuit. Figure 15 illustrates the High Gain switched LC converter’s experimental configuration. The DC source provides the input 2V DC supply. The TMS320F28335 microcontroller sends switching pulses to the driving circuit. Thus, the power circuit depicted in Figure 16 yields an output voltage of 14.4V. The DSO oscilloscope is used to measure the converter’s output voltage.



Fig. 15. Experimental Setup

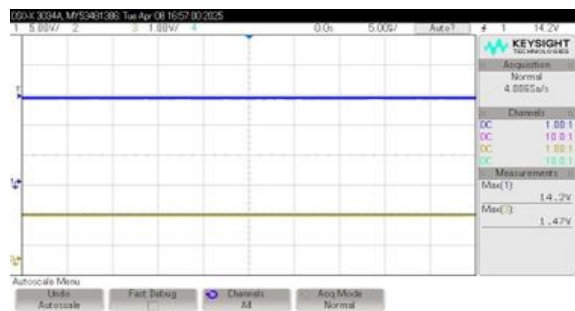


Fig. 16. Output Voltage of Proposed Converter

VII. CONCLUSION

A new modified LC converter with high gain is proposed and implemented. This structure is a combination of switched inductor and switched capacitor cells. When compared to other boost DC-DC converters, the suggested converter has higher gain and lower output ripple voltage. Simulation and analysis of the proposed converter are performed.

Based on the simulation, it can be observed that the High Gain switched LC converter achieves an efficiency of 90% for an output power of 200W. From tBecause of these characteristics, the topology that is being shown is a great interface for photovoltaic applications. When tested with an input voltage of 2 V, the converter's ability to raise the output to a regulated value of 14 V validated its suitability for high-gain applications. The control and pulse generation were implemented using a TMS320F28335 DSP board, which provided the switching de- vices with accurate PWM gate signals. This high-performance digital controller ensured accurate duty cycle modulation, fast dynamic response, and stable voltage regulation under a range of load conditions. Because of its high voltage gain, compact size, and integration of digital control, the proposed converter architecture is an excellent power interface choice for photo- voltaic energy systems and distributed energy resources when high step-up DC conversion is required.

REFERENCES

- [1] Aakash Singh” Analysis and Design of switched LC converter with reduced stress for photovoltaic applications”, IEEE Transactions on Industrial Applications, VOL. 55, NO. 5, Seotember/October 2023.
- [2] P Kumar, “Z-network plus switched capacitor boost DC-DC converter”,
- [3] IEEE Journal of emerging topics in industrial electronics,2021.
- [4] SVK Naresh,”A Novel High Quadratic Gain Boost Converter for Fuel Cell Electric Vehicle Applications,” IEEE Journal of emerging topics in industrial electronics, 2023.
- [5] Shima Sadaf, M. S. Bhaskar, M. Meraj, Atif Iqbal, Nasser Al-Emadi,” Transformer-less Boost Converter with Reduced Voltage Stress for High Voltage Step-Up Applications”, IEEE Transactions on Power Electronics, vol.69, Issues 2,2022.
- [6] K. I. Hwu and Y. T. Yau,” High step-up converter based on coupling inductor and bootstrap capacitors with active clamping”, IEEE Trans- actions on Power Electronics, vol. 29, no. 6, pp. 2655–2660, Jun. 2020.
- [7] S. M. Chen, T. J. Liang, L.S. Yang, and J. F. Chen,” A cascaded high step-up DC-DC converter with single switch for microsource applications”, IEEE Transactions on Power Electronics, vol. 26, no. 4, pp. 1146–1153, Apr. 2019.
- [8] S. Lee and H. Do,” Quadratic boost DC-DC converter with high voltage gain and reduced voltage stresses”, IEEE Transactions on Power Electronics, vol. 34, no. 3, pp. 2397–2404, Mar. 2019.
- [9] Axelrod and Y. Berkovich,” Switched-Capacitor/Switched-Inductor structures for getting transformerless Hybrid DC-DC PWM Converters”, IEEE Transactions on Circuits and Systems, vol. 55, NO. 2, MARCH 2019.